

**2018**



**25<sup>th</sup> Congress of  
International Federation for  
Heat Treatment and Surface Engineering**

*11-14 September 2018 | Xi'an China*

***PROCEEDINGS***



Organized by Chinese Heat Treatment Society (CHTS)

# 25<sup>th</sup> IFHTSE CONGRESS PROCEEDINGS

11-14 September 2018

Xi'an China



Chinese Heat Treatment Society

*Tel: +86 (0) 10 6292 0613 • Email: [chts@chts.org.cn](mailto:chts@chts.org.cn) • Web: [www.chts.org.cn](http://www.chts.org.cn)*

*Add: 18 Xueqing Rd., Beijing, China*

Elevated temperature wear behaviour of rare earth modified WC12Co coating.....	492
Effect of mechanical alloying speed on properties of CNTs-SiC/Ni laser cladding coating.....	492

### **Modelling and Simulation**

Numerical simulation of heat treatment and its engineering application.....	493
Heat treatment simulation for low pressure super carburizing process.....	494
Heat transfer coefficient model of large cross section steel bar during water cooling process.....	495
Modelling on quenching precipitation of Al-Cu-Cd alloy.....	496
Diffusion simulation in SUS 430 stainless steel interconnect with a MnCu coating at 800 °C.....	497
Application of universal function approximator to predict HTC during quenching.....	498
Influence of circular workpieces configurations on temperature field of vacuum heating process.....	498
Heat transfer, microstructure evolution and stress development in a quenched 403 stainless steel forging.....	499
Microstructural evolution of a steam turbine rotor subjected to a water quenching process: numerical simulation and experimental verification.....	499
Modeling carburization heat treatment processes of steel camshaft in marine engine using commercial software DANTE.....	500
Superalloy in synchronization powder feeding laser cladding.....	500
Microstructure-based mesoscopic modeling of deformation behavior of dual-phase steels using crystal plasticity finite element method.....	501
Effect of residual stress on indentation and rebound hardness measurement.....	502
Isothermal phase transition kinetics of TC11 titanium alloy.....	504
Stress relaxation performance and thermal calibration of TC4 titanium alloy at high temperature.....	506
Numerical and experimental investigation into the austenite decomposition kinetics of 50Cr5NiMoV steel.....	508
Three-dimensional numerical simulation of temperature field of Ni based cellular automaton modeling of nitriding process in pure iron.....	509
Design method fin-tube heat exchange based on numerical simulation.....	509

### **Characterization and Evaluation of Residual Stress; Shot Peening Technology**

Evaluation of internal residual stress in rolled pure copper plate.....	510
Effect of laser shock processing and aluminizing on microstructure and high temperature creep properties of 321 stainless steel.....	511
Research progress and application of residual stress neutron diffractometer at CMRR.....	512
Investigation on the thermostability of residual stress and microstructure in shot peened SAF 2507 duplex stainless steel.....	513
Evaluating the fatigue cracking risk of surface strengthened 50CrMnMoVNb spring steel with abnormal life time distribution.....	514

## Numerical simulation of heat treatment and its engineering application

Jianfeng Gu

(Institute of Materials Modification and Modeling, School of Materials Science and Engineering,  
Shanghai Jiao Tong University, Shanghai 200240, PR China)

gujf@sjtu.edu.cn

**Abstract:** Numerical simulation of heat treatment can provide strong support for the design and optimization of heat treatment process and equipment, which has been more and more accepted and valued in engineering practice, and has been more and more applied in engineering machinery, high-speed railway, nuclear power, automobile, aerospace and other fields.

The main characteristics of heat treatment numerical simulation have firstly been summarized, and related important models have briefly been listed. The models include: 1) iso-conversional model of steels austenitizing heating, 2) transformation calculation model of steels during cooling process, 3) prediction model of mechanical property of quenched steels, 4) microstructure and property evolution model of steels during tempering process, 5) microstructure and property evolution model of non-ferrous alloys during aging process, 6) multiple field coupling model of induction heating process, 7) multiple field coupling model of steels during quenching process, and etc.

The heat treatment simulation software Thermal Prophet<sup>®</sup> developed by author and his research group has been introduced in the second part. Some typical engineering application cases have been carried out and discussed, including 1) quenching and tempering of the integration head forging for nuclear power, 2) induction burns and tempering repair of generator rotor for nuclear power, 3) carburizing and quenching of wind power gears, 4) quenching of large steel modules for plastic dies.

Finally, the numerical simulation cases of heat treatment using computational fluid dynamics(CFD) are introduced, including 1) post-weld stress relief heat treatment of nuclear welded rotor, 2) flow field calculation and design of large quenching tank, 3) vacuum heating and gas quenching, etc.

In general, heat treatment numerical simulation is a common and key frontier technology and also a core content in the realization of heat treatment virtual manufacturing, and its potential will be given full play in near future.

**Keywords:** heat treatment, numerical simulation, microstructure and property, computational fluid dynamics, process and equipment

## Heat treatment simulation for low pressure super carburizing process

Tsuyoshi Sugimoto<sup>1,2</sup>, Dongying Ju<sup>2</sup>

(1. Nissan Motor Co., Ltd.; 2. Saitama Institute of Technology)

tsuyoshi-sugimoto@mail.nissan.co.jp

**Abstract:** Carburizing heat treatment is well used to increase the strength of gears and automobile drivetrain parts. In particular, when high fatigue strength is required, super carburization or carbonitriding may be used to improve the surface hardness and temper softening resistance. Over saturate carburizing as called super carburizing can be used in a conventional ordinary carburizing furnace and investment of new gas supply equipment is unnecessary, while there are problems such as controlling precipitation of cementite and securing hardenability of the surface, etc. Also, problems such as secondary quenching In order to control the material structure, its quality prediction method becomes important.

In recent years the low pressure carburizing method has been widely used and the possibility of making super carburizing inexpensive has been expanding. However, when super carburizing is performed by low pressure carburizing, reticulated cementite occurs at the edge of the part, there is a problem such as local increase of carbon concentration distribution and toughness. In this study, we tried to formulate precipitation of precipitation when super carburizing was performed on steel parts using a vacuum carburizing furnace, formulated the surface hardness distribution, and tried to calculate the hardness and cementite precipitation size distribution. We established a quality distribution prediction method and tried to study these issues.

Super carburizing heat treatment of the cylindrical test piece and gear parts was carried out by the secondary quenching method by vacuum carburization. After heating and secondary precipitation conditions were changed to several kinds, after quenching, macrostructure, hardness distribution, and precipitation state of precipitates after quenching were investigated with a microscope, hardness meter and XRD.

At the same time, the state of low pressure carburizing was calculated by the carburizing heat treatment simulation using SFTC DEFORM - HT 3D and the situation of precipitation of cementite at the time of the secondary precipitation was predicted.

Carbonizing heat treatment simulation for low pressure carburization and precipitation was carried out to investigate the precipitation situation and hardness distribution of cementite after carburization. By examining the primary carburization conditions and the precipitation temperature in the secondary precipitation, it was possible to derive the condition that maximizes the hardness of the surface after finely dispersing cementite. We also conducted a deformation calculation on the mother phase to investigate the prediction method of heat treatment deformation and residual stress in low pressure super carburizing.

By conducting the condition derivation by carburizing heat treatment simulation at the time of low pressure super carburization, prediction method of carbon concentration non uniformity, net mesh precipitation of meshes, which is a problem of the same construction method, was studied. By using this method, it is possible to investigate material conditions and heat treatment conditions to suppress these problems.

**Keywords:** super carburizing, precipitation, heat treatment simulation

## Heat transfer coefficient model of large cross section steel bar during water cooling process

Liwen Zhang, Wenfei Shen, Chi Zhang, Yan Cui

(School of Materials Science and Engineering, Dalian University of Technology, Dalian 116024, China)  
commat@mail.dlut.edu.cn

**Abstract:** Owing to the size effect, the quality of large cross section steel bar decreases with increasing size. To improve the quality of large steel bar, an effective online heat treatment is needed after finishing rolling. Water cooling process which can save cost and be free of pollution is often used in the heat treatment. During cooling process, too fast or too slow cooling rate may be bad for the final property of production. The quality of steel bar can be greatly improved by an appropriate cooling rate, by which fine microstructure and dispersion precipitation can be obtained. Therefore, the controlling of cooling rate is very important. However, the heat transfer coefficient of large steel bar during water cooling process is not clearly reported previously. Therefore, a mathematic model which describes the relationship between heat transfer coefficient and various operation parameters is necessary.

In order to obtain the mathematic model, a series of experiments were conducted. The temperatures of steel bar were measured in different operation parameters, such as water pressures, water fluxes and sizes of steel bar. Then, the heat transfer coefficient was calculated using finite element (FE) method. According to the analysis results, a mathematic model was established by nonlinear regression method. Finally, the established mathematic model was verified by actual production process.

The experiments results show that the water pressure and size of steel bar have no obvious effect on the heat transfer coefficient. And the water flux can greatly affect the heat transfer coefficient. Based on the experimental data, the mathematic model which describes the heat transfer coefficient with different operation parameters was established in power function, as shown in Fig.1. It can be seen that the heat transfer coefficient increases with the increasing of water flux. And the experimental data is distributed near the fitting curve illustrating that the fitting effect is good. Using FE method, the mathematic model was successfully applied into actual water cooling process. The predicted temperature of steel bar agree well with the experimental results, as shown in Fig.2, which indicates that the established mathematic model is acceptable under the experimental conditions.

**Keywords:** heat transfer coefficient, mathematic model, water cooling process, large cross section steel bar

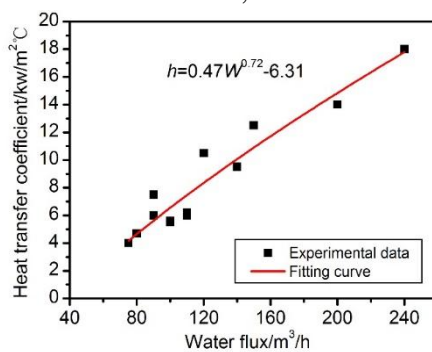


Fig.1

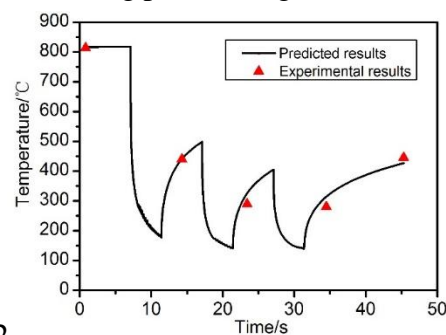


Fig.2

Fig.1 The fitting curve of heat transfer coefficient

Fig.2 Comparison of predicted temperature and experimental results

## Modelling on quenching precipitation of Al-Cu-Cd alloy

Sheng Luo<sup>1,3</sup>, Gang Wang<sup>1,2</sup>, Yisen Hu<sup>1,2</sup>, Yiming Rong<sup>1,3</sup>

- (1. State Key Laboratory of Tribology & Institute of Manufacturing Engineering, Tsinghua University;  
2. Beijing Key Lab of Precision/Ultra-precision Manufacturing Equipments and Control, Tsinghua University;  
3. Mechanical and Energy Engineering Department, Southern University of Science and Technology)

gwang@mail.tsinghua.edu.cn

**Abstract:** The mechanical properties of the Al-Cu alloy after T6 heat treatment mainly depend on the quenching rate and the aging treatment conditions. Considering the different quenching rates and cooling conditions of large-scale components, quench precipitate has a considerable impact on the yield strength of the aging process. Coupling quenching factor analysis (QFA) and precipitation strengthening model (PSM) are used in this paper to establish the relationship between copper content ( $C_m$ ) and quenching factor ( $Q$ ), and to propose a complete prediction method for yield strength of quenching-aging dynamic process, which can describe the yield strength during aging under different quenching conditions. Furthermore, the precipitation strengthening model (PSM) focuses on the effect of aging conditions on the metal properties. This paper presents a coupling model for predicting the variation of yield strength of Al-Cu-Cd alloys. The Al-Cu-Cd alloy was treated under different quenching rates and aging time. The experimental results were compared with the modelling data. The results showed that the model prediction results can correlate well with the Al-Cu-Cd alloy under the rapid quenching rate, and have a good prediction of the peak aging when the cooling rate is lower.

In this paper, the modified QFA model and the PSW model are coupled. The results are compared with the experimental results and get the following conclusions: 1) The modified QFA model can accurately calculate the yield strength of the alloy at the peak aging due to the  $\sigma_{\min}$  variation with temperature, and the maximum error of the prediction result is within 5%. 2) The PSW model has good accuracy for rapid quenching, but for slower rate quenching, due to the model does not consider the impact of the precipitates during quenching, so there are larger errors, the correction of PSW must take into account the influence of precipitates during quenching. In addition, due to the presence of precipitates in the quenching, the content of Cu in the matrix is reduced, resulting in the change in the diffusion coefficient, resulting in the peak aging time calculated by the model precluded sooner than the experimental data. 3) Through analysis, we can appropriately adjust the relationship between the predicted value of the PSW model and the experimental value, establish the relationship between the  $Q$  value and the  $C_m$  value to a certain extent, and use the PSW model to calculate the data from a series of models and experimental data through computer repetitive calculations. In the comparison, a suitable  $C_m$  value is obtained. Through the fitting of the 5 groups of data, the relationship between the  $Q$  value and the  $C_m$  value was found as shown in equation.  $Q=k(e^{A(C_0-C_m)}-1)$ , Where  $k=13.41$ ,  $A=362.7$ , which are constants. It is essential to modified the PSM, which should take precipitate during quenching and the effect of diffusion coefficient into account, and need more experimental data to verify the relationship of  $Q$  and  $C_m$ .

**Keywords:** quenching factor analysis, precipitation strengthening model, yield strength, Al-Cu-Cd alloy

**Table 1 Comparison of peak predicted results with experimental results**

Quench method	10%ucon	80 °C W	Wind	Air	100 °C F	F
measured	458	446	421	315	215	65
predicted	456	448	428	304	225	66
error	0.4%	0.4%	1.6%	3.5%	4.6%	1.5%

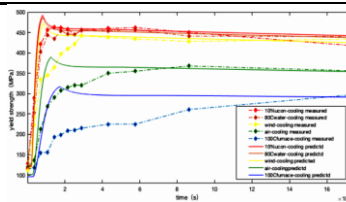


Fig.1 Fitting of experimental data and model data

## **Diffusion simulation in SUS 430 stainless steel interconnect with a MnCu coating at 800 °C**

Kang Yuan<sup>1</sup>, Shujiang Geng<sup>2</sup>

(1. BGRIMM Technology Group; 2. Northeastern University)

bityuankang@126.com

**Abstract:** As the development of solid oxide fuel cells (SOFCs) moves to medium-high temperature ranges (700-800 °C), cheap stainless steels can use as the interconnects. At such high temperatures, Cr evaporation from the stainless steels is still a problem which causes Cr poisoning of the fuel cells. In our study, a MnCu metallic coating was sputtered onto the interconnect surface followed by hot oxidation treatment to in-situ form protective diffusion-blocking oxide layer. The interconnect used was a typical SUS 430 stainless steel and the sputtered MnCu coating was around 7 μm thick. The oxidation was conducted in air at 800 °C. The basic mechanism of the formation of the oxide layers on the coated steel has been studied in S. Geng's previous work. To step further for understanding how the elements diffuse in the steel-MnCu system, a homogenization diffusion model was applied to simulate the elemental diffusing behavior. As the experimental results has shown that the first 10 min oxidation was critically important to form protective oxide layers, the model focused on the microstructure and element profile development in this period. According to our simulation, diffusion of Fe and Cr from the steel substrate to the MnCu coating occurred. The diffusion of Fe was faster, which agreed with the experiment of that Fe was detected in the middle MnCu oxides. Cr diffused relatively slower and was mainly concentrated at the interface of the substrate and MnCu coating, resulting in the formation of chromia near the interface. Inwards diffusion of Mn and Cu from the coating to the substrate also took place. Concentration peak of Mn was successfully predicted to be formed at the substrate - coating interface. Thermodynamic theory indicates that activity but not concentration commands the diffusion direction of the elements. The diffusion modeling results helped to explain the oxidation process of the MnCu coated SUS 430 stainless steel interconnect.

**Keywords:** simulation, MnCu coating, interconnect, diffusion, oxidation

## **Application of universal function approximator to predict HTC during quenching**

Imre Felde, Sandor Szenasi, Zoltan Fried, Marta Seebauer  
(Obuda University)  
imre.felde@gmail.com

**Abstract:** To achieve the desired performance of object to be heat treated, it is necessary to know the heat transfer coefficient (HTC) which describes the amount of heat exchange between the work piece and the cooling medium. The task of HTC's prediction belongs to the Inverse Heat Transfer Problems (IHCP) which can not be solved by direct numerical methods. The several methods used to solve the IHCP are based on heuristic search algorithms, like Genetic Algorithms or Particle Swarm Optimization, and other methods using swarm theory. In these cases, each instance (chromosome/particle) represents a possible HTC function, and the fitness value is presented as the squared difference of the measured and the simulated cooling curves using the evaluated HTC values. The results of these methods are promising, however the processes need hundreds of instances and thousands of iterations. Therefore, the number of fitness function evaluations (which needs an entire simulation of cooling down) is significantly high, making the process very timeconsuming. This paper suggests a special application of artificial neural networks (ANN), the universal function aproximator. After the time-consuming training process, this network is capable of giving prompt estimations about the nature of the HTC function sought. This estimation would be a useful input for additional fine-tuning algorithms and finally for complex simulation of heat treatment operations.

**Keywords:** inverse heat conduction problem, artificial neural network, universal function aproximator

## **Influence of circular workpieces configurations on temperature field of vacuum heating process**

Jing Liu, Jiadong Li, Haojie Wang, Yong Li, Yong Tian, Zhaodong Wang

(State Key Laboratory of Rolling and Automation, Northeastern University, Shenyang 110004, China)

**Abstract:** The configurations of workpieces determine the view factors between workpieces surfaces, which affects the radiation heat transfer between surfaces of the loads. Vacuum heating processes of workpieces with two typical shape, round bar and disc shape, are studied. In order to achieve high-efficient and uniform radiation heat transfer, finite element method has been applied to calculate the temperature field of the loads with different arrays. The effects of arrays of workpieces on the heating rate and temperature uniformity are investigated. The results indicated that under the same heating process, round bar in aligned arrangement and the disc in vertical arrangement can effectively reduce radiation dark zone, improve heating uniformity and increase heating efficiency. The simulation results have directive significance for the configurations of circular workpieces, such as gears, shafts, bearings and nozzles, in the heating zone of vacuum furnace.

**Keywords:** circular workpieces, loads configurations, vacuum heating, finite element method, temperature field

## **Heat transfer, microstructure evolution and stress development in a quenched 403 stainless steel forging**

Youxin Zhu<sup>1</sup>, Mengnie V. Li<sup>1</sup>, Hengyong Bu<sup>1</sup>, Zisheng Zhang<sup>2</sup>, Xiaoguang Zhao<sup>2</sup>  
(1. Kunming University of Science and Technology, Kunming Yunnan 650093, China;  
2. Guizhou Aerospace Xinli Forging & Casting Co, Zunyi Guizhou563003, China)  
mvictorli@outlook.com

**Abstract:** Coupled thermo-mechanical analysis is conducted to simulate the heat transfer and residual stresses development in the quenching of a manhole base forging for a nuclear power plant. The manhole base forging is made of 403 stainless steel. Finite element analysis code ABAQUS is used with coupled temperature-displacement elements. Thermophysical and mechanical properties of 403 stainless steel are computed using JMatPro with correspondence to the microstructure of the material. User subroutines are developed to prescribe the heat transfer boundary conditions and to predict microstructure evolution, heat absorption and release due to phase transformations. Mechanical properties are estimated based on the predicted microstructure, and then compared with experimental test results. Study shows that there is a temperature difference of more than 300 °C between surface and inside when furnace temperature reaches the set austenization temperature of 970 °C upon heating for 4 hours from room temperature. Holding at 970 °C for 1.5 h, temperature in the manhole base forging is still about 20-100 °C below 970 °C, which yields inhomogeneous microstructure with various amount of residual M<sub>23</sub>C<sub>6</sub> carbides.

During quenching, cooling rates between 800-500 °C varies from around 15 °C/s at surface to 0.3 °C/s inside, giving rise to increased amount of M<sub>23</sub>C<sub>6</sub> carbide precipitates from surface to inside in the matrix of martensite.

**Keywords:** 403 stainless steel, quenching, microstructure evolution

## **Microstructural evolution of a steam turbine rotor subjected to a water quenching process: numerical simulation and experimental verification**

Chuan Wu  
(Tianjin University of Technology and Education)  
zjkwuchuan@126.com

**Abstract:** Cr-Ni-Mo-V steam turbine rotors, have been widely used as key parts in power plants. In this study, a coupled thermomechano–metallurgical model was proposed to simulate the phase transformation and transformation-induced plasticity (TRIP) of a 30Cr2Ni4MoV steam turbine rotor during a water quenching process, which was solved by a UMAT subroutine in ABAQUS. The thermal dilation, heat generation from plastic work, transformation latent heat, phase transformation kinetics, and TRIP were considered in the model. The thermomechano part of the model was used to predict the evolution of temperature, strain, and residual stress in the rotor. The metallurgical part dealt with the phase transformation that occurred during the quenching process. Constitutive models of phase transformations (austenite to pearlite, austenite to bainite, and austenite to martensite) and TRIP were developed. To verify the accuracy of the model, experimental data from the literature were adopted and compared with the predicted results, which showed that the model was reliable and accurate. Then, the model was utilized to predict the temperature variation, dimensional change, minimum austenitization time, residual stress, TRIP, and volume fractions of each phase. It was concluded that this model could be a useful computational tool in the design of heat treatment routines of steam turbine rotors.

**Keywords:** thermomechano-metallurgical model, UMAT subroutine, microstructural evolution

## **Modeling carburization heat treatment processes of steel camshaft in marine engine using commercial software DANTE**

Jianpin Li<sup>1</sup>, Qiang Wang<sup>1</sup>, Liping Cao<sup>2</sup>, Xiaoyun Zhang<sup>2</sup>

(1. Beijing Auto CAE Technology Co., Ltd.; 2. Shaanxi Diesel Engine Heavy Industry Ltd.)

**Abstract:** The steel camshaft is the core running part in marine engine. The surface hardness and dimension precision have the great influence on the service quality and fatigue life. In present paper, the heat treatment process of a camshaft made of carburized steel AISI 5110 is modeled using the commercial heat treatment simulation software DANTE. With the understanding of complex interaction of carbon diffusion, thermal history, microstructure evolution and mechanical response, the heat treatment process of camshaft is expected to be optimized for improved part performance. During carburization and quench hardening processes for steel components, both carbon gradient, thermal gradient and phase transformations in the part contribute to hardness and microstructure in the final part. The camshaft is carburized and then followed by an immersion oil quenching process. The final carbon gradient, microstructure distribution and hardness are predicted by dint of computer modelling. The relation of the carbon distribution, thermal gradient, and phase transformations during quenching is studied through the modeling example. The results show the non-uniform hardness distribution on the part surface due to the different carbon distribution and thermal history of complex section geometry. Furthermore, the distortion of camshaft in every stage of heat treatment is predicted by considering the effect of thermal gradient and phase transformations. In general, the radial direction shows the bend distortion while the axial direction has an elongation. The cause of distortion is discussed. Both measured hardness and distortion are adopted to validate the simulation results. Based on the simulation analysis, improved heat treatment processes for controlling distortion and eliminating the soft zone are suggested.

**Keywords:** carburization heat treatment simulation, DANTE software, Auto CAE

## **Superalloy in synchronization powder feeding laser cladding**

Longzhi Zhao

(East China Jiaotong University)

**Abstract:** A Three-dimensional numerical model is developed on the basis principle of synchronization powder feeding laser cladding. The model, which takes the heating of powder particles and the shielding effect of laser beam in the powder feeding process into account. The temperature field at different time in the process of cladding is calculated, and the distribution of the temperature field and the feature of the geometry of the molten pool are analyzed. The results show that: With the increase of heating time, the laser energy density tends to be stable, and the energy of the system tends to be balanced. At the 0.7 s time, the pool reaches the maximum, and the pool shape and temperature field tend to be stable. Experiments with different power are performed to validate the calculated results. The calculating coating outline, width, height, as well as surface profile of coating, agree with the experimental ones. So the reliability of the model is proved.

**Keywords:** laser cladding, numerical simulation, temperature field, the molten pool

## Microstructure-based mesoscopic modeling of deformation behavior of dual-phase steels using crystal plasticity finite element method

Gang Shen<sup>1</sup>, Chengwu Zheng<sup>2</sup>, Jianfeng Gu<sup>1</sup>

(1. Shanghai Jiao Tong University;

2. Shenyang National Laboratory for Materials Science, Institute of Metal Research)

jackshen2018@sjtu.edu.cn

**Abstract:** In this study, microstructure-based representative volume element (RVE) modeling of the material deformation of a dual-phase (DP) steel under uniaxial tension is performed using crystal plasticity finite element method (CPFEM) to quantitatively describe the plastic deformation behavior inside the two-phase structure at grain scale. In the RVE model, the initial geometry of the DP microstructure including the grain topology is created directly from real metallographic images based on a digital material representation algorithm. Periodic boundary conditions are used for CPFEM analysis. Macroscale material flow curves are statistically obtained from the CPFEM simulation results based on the first order homogenization strategy. A series of RVE models with various sizes are firstly created and calculated to determine the critical RVE size for the investigated DP microstructure by convergence evaluations of the extracted flow curves. Typical RVE models larger than the critical size are then used to evaluate the deformation behavior of the investigated DP microstructure under uniaxial tension. Finally, microstructure deformation patterns and flow curves are compared with experimental observations. Simulation results show that macroscale material properties in terms of flow behaviors represented by the selected RVE model are strongly influenced by the RVE size when the RVE model is small. A Critical RVE size exists, which is correlated with the initial microstructure morphology, such as the size and distribution of ferrite grains and martensite islands. As the RVE size exceeds the critical value, the represented material properties converge to the actual values, which means that the selected RVE model larger than the critical size can be applicable for reliable simulations. Simulation results also reveal the occurrence of deformation heterogeneity, such as strain and stress partitioning and deformation banding, within the deformed microstructure during uniaxial tension of the DP steel. Significant strain localization is formed within the ferrite matrix producing narrow deformation bands throughout the microstructure. Meanwhile, high stresses are found within the martensite islands during deformation. Deformation heterogeneity is also found within individual ferrite grains due to the existence of crystallographic orientation gradient between neighboring grains. The simulated distribution of deformation bands, locations of strain concentration as well as the strain-stress curve are in good accordance with experimental observations, which confirms the validation of the proposed modeling approach.

**Keywords:** dual-phase steel, microstructure-based modeling, representative volume element, crystal plasticity, microstructure deformation, mesoscale simulation

## Effect of residual stress on indentation and rebound hardness measurement

Daming Tong, Jianfeng Gu

(Institute of Materials Modification and Modelling, School of Materials Science and Engineering,  
Shanghai Jiao Tong University)

gujf@sjtu.edu.cn

**Abstract:** Hardness is one of the important indicators of the mechanical property and the most easy to use means for quality inspection for heat-treated components. Indentation and rebound methods are commonly used in hardness testing and have their own particular features. Residual stress is inevitable after heat treatment and will affect the mechanical behavior of components. The effect of residual stress on hardness measurement is an important concerned topic that has been discussed extensively over last decades.

In this work, a universal testing machine is used to apply a uniaxial force to as-tempered 20Cr2Ni4MoV steel sample, as shown in Fig.1. The middle part and the end of the sample are chosen for the hardness test under tensile stress and compressive stress, respectively. The portable ultrasonic impedance (UCI) hardness instrument and Leeb hardness instrument are used to test the hardness of the sample with different applied stress. The UCI hardness is obtained by measuring the indentation area on the sample, while the Leeb hardness is obtained by measuring the rebound speed of the impact body. For comparison, the value of UCI and Leeb are transformed into Vicker hardness value in this work. The distribution of the residual stress on the sample with external applied stresses is analyzed by FEM method. Fig.2 and Fig.3 show the model and distribution of residual stress with applied tensile and compressive load of 300 MPa respectively. When tensile stress is applied, the maximum stress of the sample is at the chamfer. The magnitude of  $\sigma_x$  (stress component on the direction of applied tensile stress) at the middle part of the sample is the same as applied stress and relatively uniform. When compressive stress is applied, the magnitude of  $\sigma_y$  (stress component on the direction of applied compressive stress) at the end of the sample is the same as applied stress and relatively uniform. The result indicates that the selected test surface is appropriate for the hardness measurement.

Fig.4 shows Leeb and UCI hardness changing with applied compressive and tensile stress. It can be inferred that the residual stress has little effect on UCI hardness due to the large indentation load. The influence of residual stress on UCI harness reduces with the increasing of the indentation area. In practice, in order to acquire precise hardness value, it is essential to use high indentation load to produce enough plastic deformation. The residual stress has a significant impact on Leeb hardness. The rebound speed of the impact body is affected by elastic modulus which is dependent on the atomic distance. The atomic distance increases with the increasing of the tensile stress, which result in the decreasing of elastic modulus. The Leeb hardness increases 23 HV (equivalent Vicker hardness) when the compressive stress increases from 0 to 400 MPa, while decreases 43 HV when the tensile stress increases from 0 to 700 MPa. It can be concluded that the Leeb hardness is more sensitive to residual stress than UCI hardness. Therefore, it is possible to qualitatively evaluate the residual stress of the component using rebound hardness measurement.

**Keywords:** indentation hardness, rebound hardness, residual stress, Leeb hardness

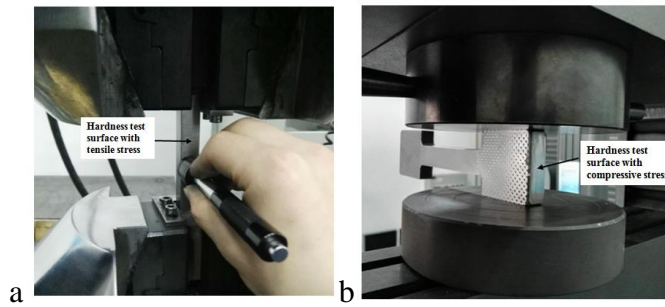


Fig.1 Schematic of hardness test under different applied load: (a) tensile stress and (b) compressive stress

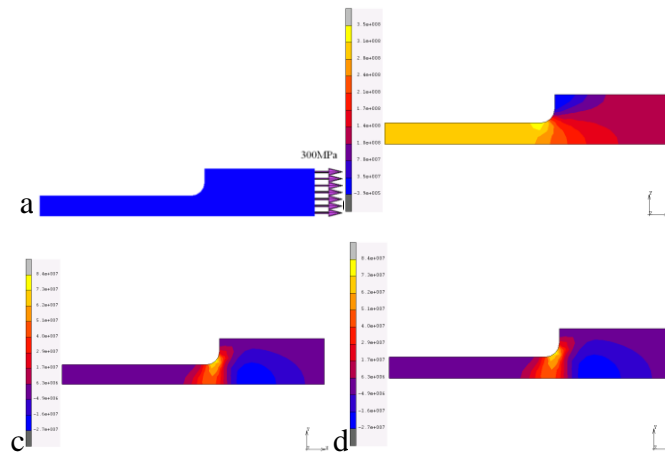


Fig.2 The simulated stress distribution in a sample with applied tensile load of 300 MPa: (a) model; (b)  $\sigma_x$ ; (c)  $\sigma_y$ ; (d)  $\sigma_z$

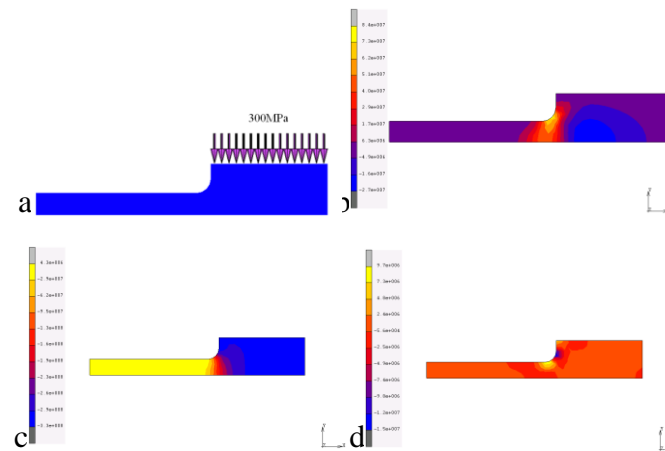


Fig.3 The simulated stress distribution in a sample with applied compressive load of 300 MPa: (a) model; (b)  $\sigma_x$ ; (c)  $\sigma_y$ ; (d)  $\sigma_z$

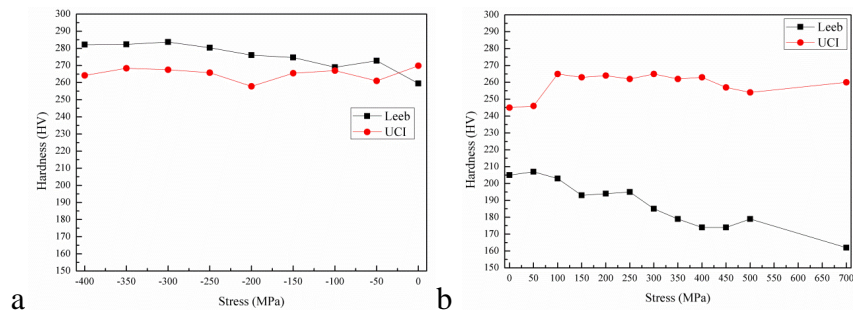


Fig.4 Leeb and UCI hardness with different applied loads: (a) compressive and (b) tensile stress

## Isothermal phase transition kinetics of TC11 titanium alloy

Lifang Zhang<sup>1</sup>, Yong Liu<sup>1,2</sup>, Meng Yao<sup>1</sup>, Zhonghong Lai<sup>3</sup>, Jingchuan Zhu<sup>1,2</sup>

(1. School of Material Science and Engineering, Harbin Institute of Technology, Harbin 150001, China;

2. National Key Laboratory for Precision Hot Processing of Metals, Harbin Institute of Technology, Harbin 150001, China;

3. The Analysis and Testing Center of Harbin Institute of Technology, Harbin 150001, China)

flyido@163.com

**Abstract:** At present, there are few studies on the thermodynamics and kinetics of phase transformation of TC11 titanium alloys. The formulation of heat treatment processes is mostly empirical or experimental so that it is difficult to explain the specific reasons for the best selection of temperature and time. This will also increase the number of experiments, causing waste of human and material resources. In addition, the continuous development of material calculations with the help of material genomes and big data technologies makes the studies of thermodynamics and kinetics particularly important. In this paper, the isothermal phase transition test of the alloy is studied to research its behavior based on the phase diagram thermodynamic calculation of TC11 titanium alloy. And the time required for the alloy phase transition to equilibrium at different temperatures is obtained. Besides, this paper established the isotherm phase transformation kinetic model for  $\alpha \rightarrow \beta$  heating at different temperatures based on Avrami equation. The results show that the heat treatment temperature above 950 °C should be the first choice in the process of the actual heat treatment process, and the holding time should be about 40 min or longer.

Fig.1 shows quantitative relationship between volume fraction of  $\alpha$ -phase and holding time at different temperatures. Comprehensively comparing the trend of the  $\alpha$ -phase volume fraction of the microstructure of the alloy after incubation at various holding temperatures, it can be seen that the higher the isothermal temperature, the faster the phase transition and the shorter the time required to reach equilibrium.

Fig.2 shows the effect of holding time at different temperatures on the volume fraction of  $\beta$  phase that have transformed. It can be seen that the increasing rate of  $\beta$  phase content is firstly slow at each temperature and gradually increases with the extension of holding time. When the phase transition is close to equilibrium, the rate increasing of  $\beta$  phase decreases again, and with the increase of heat treatment temperature, the rate increase of  $\beta$  phase content become faster.

Fig.3 shows the heating isothermal transition TTT chart of TC11 titanium alloy. The time corresponding to the selected  $\beta$  phase transformation volume fraction is 1%, which is the start time of transition. The figure can predict the isothermal transformation of the alloy at a certain temperature, the length of the incubation period and when the conversion is completed, providing a reference for the choice of time in the heat treatment process.

The following is isothermal phase transition kinetic model at different temperatures. The Avrami index “n” of the alloy at each holding temperature are all about two. It can be seen that as the isothermal temperature increases, the value of “n” increases, and the lower the isothermal temperature, the greater the proportion of non-uniform nucleation. 700 °C:  $f=1-\exp(-5.0321 \times 10^{-4} t^{1.70999})$ ; 800 °C:  $f=1-\exp(-6.9960 \times 10^{-4} t^{1.74236})$ ; 900 °C:  $f=1-\exp(-9.4565 \times 10^{-4} t^{1.88962})$ ; 950 °C:  $f=1-\exp(-14.063 \times 10^{-4} t^{2.11704})$ .

The higher the holding temperature, the faster the  $\alpha$  phase content drops. The equilibrium time of alloy phase transition at 700, 800, 900, and 950 °C are 180, 150, 90 and 40 min.

The Avrami index of the alloy at different temperatures are all about 2, and the value of “n” increase as the isothermal temperature rises, which means that the lower the isothermal temperature, the greater the proportion of inhomogeneous nucleation.

The heat treatment temperature above 950 °C should be preferred in the process of the actual heat treatment process, and the holding time should be about 40 minutes or longer.

**Keywords:** TC11 titanium alloy, isothermal phase transition kinetics

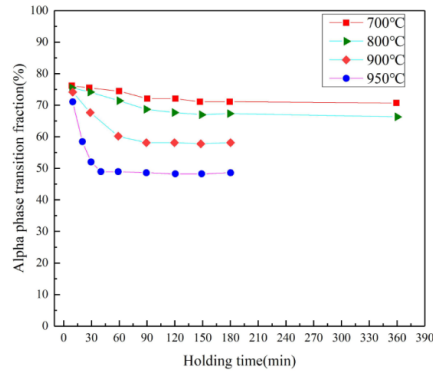


Fig.1 Effect of different holding time on volume fraction of  $\alpha$  phase at different temperatures

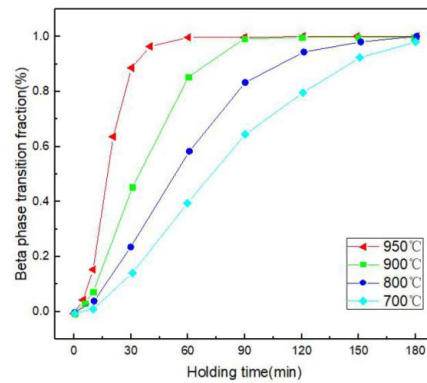


Fig.2 Non-homogeneous transition kinetics curves at different temperatures

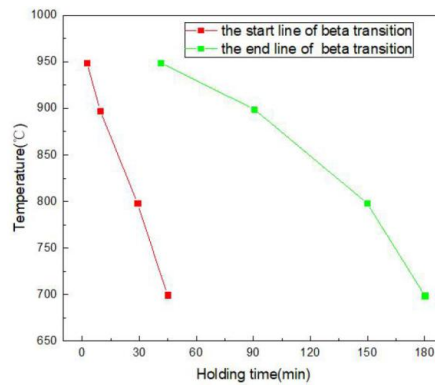


Fig.3 Heating isothermal transition TTT chart of TC11 titanium alloy

## Stress relaxation performance and thermal calibration of TC4 titanium alloy at high temperature

Quan Wang<sup>1,2</sup>, Le Lai<sup>1</sup>, Zhonghong Lai<sup>4</sup>, Yong Liu<sup>1,3</sup>, Jingchuan Zhu<sup>1,3</sup>

(1. School of Material Science and Engineering, Harbin Institute of Technology, Harbin 150001, China;

2. AECC Shenyang Engine Research Institute, Shenyang 110015, China;

3. National Key Laboratory for Precision Hot Processing of Metals, Harbin Institute of Technology, Harbin 150001, China;

4. The Analysis and Testing Center of Harbin Institute of Technology, Harbin 150001, China)  
371664718@qq.com

**Abstract:** In this paper, TC4 titanium alloy is used as the representative of the dual phase titanium alloy. The stress relaxation properties of the open ring specimen are studied at different temperatures and initial stresses. Based on this, the constitutive equation of creep plastic strain and transient stress at 700 °C are established. At the same time, the ABAQUS finite element software was used to simulate the thermal calibration process of the open ring of TC4 titanium alloy, and the microstructure and mechanical properties of the hot-formed samples at 700 °C after three-state tissue heat treatment process were compared and verified. The test results show that there is no major change in the structure and properties, and the strength, plasticity, and toughness properties keep a well comprehensive performance level.

The open ring specimens were obtained by heating to 985 °C for 30 min, followed by water-cooling, and then reheating to 940 °C for 60 min followed by air-cooling. The bending stress relaxation test was conducted according to GB/T 10120. To study the stress relaxation performance at different temperatures, stress relaxation of the open-ring specimen was performed at five temperatures (900, 800, 700, 650 and 600 °C). The finite element simulation was implemented by ABAQUS software. The open ring model was created and shown in Fig.1, and the size is shown in Fig.2. Since the open ring is axisymmetric, only half-model need to take into consideration in the simulation. In order to ensure accuracy, the grid at the ring mouth is refined when meshing, and the element type is C3D8I (8-node hexahedral linear uncoordinated simulation unit).

Stress relaxation performance of TC4 at different process is presented in Fig.3(a) and Fig.3(b). Constitutive equation of creep plasticity and transient stress at 700 °C. Comparison of curves about stress relaxation and experiment during thermoforming of opening rings are shown in Fig.4. The microstructure and mechanical properties of 700 °C hot calibration after heat treatment with the three-state structure are presented in Fig.5 and Table 1.

1) The stress relaxation curve at each temperature shows two typical stages. The rate of initial stress relaxation increases with the increase of temperature, and the gap between different temperatures decreases after the second stage.

2) The higher the initial stress is, the larger the stress relaxation rate is. However, as the stress relaxation time prolongs, the stress relaxation curves under different initial stresses tend to be the same. The simulated stress relaxation trends agree well with the experimentally measured trends.

3) The microstructure and mechanical properties of TC4 handled by 700 °C hot calibration after heat treatment with the three-state structure didn't have much difference. After the treatment, strength, plasticity and toughness properties reach a well comprehensive performance level.

**Keywords:** TC4 titanium alloy, stress relaxation, thermal calibration

**Table 1 The mechanical properties of 700 °C hot calibration**

Process	Tensile strength/MPa	Yield strength/MPa	Elongation rate/%	Multiplying strength plastic/MPa %	Impact energy/J
1	1040.5	918.4	23.07	24004.1	17.9
2	1022.0	943.6	24.07	24599.5	17.1

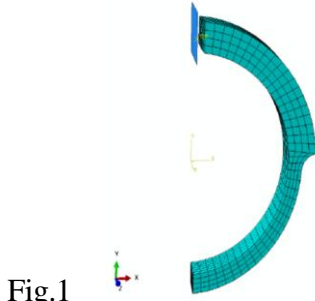


Fig.1

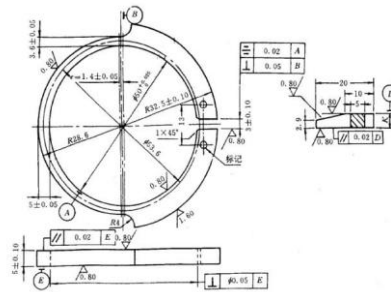


Fig.2

Fig.1 The open ring model

Fig.2 The size of specimen

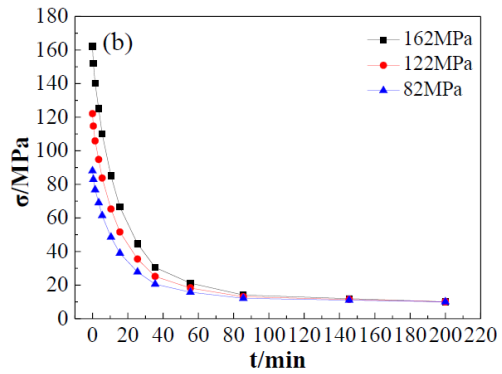
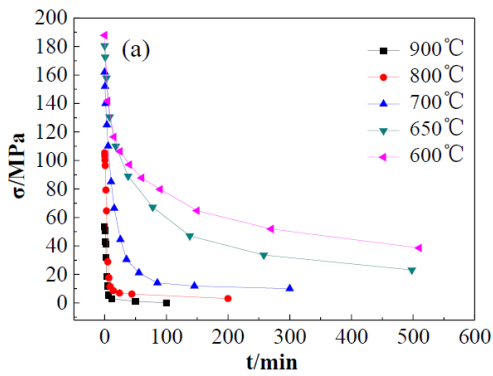


Fig.3 Stress relaxation performance of TC4: (a) different temperatures; (b) different initial stresses at 700 °C

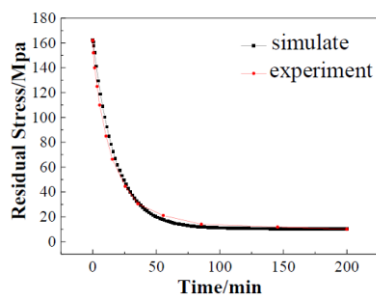


Fig.4

Fig.4 Comparison of curves about stress relaxation and experiment



Fig.5

Fig.5 The microstructure of 700 °C hot calibration

## Numerical and experimental investigation into the austenite decomposition

### kinetics of 50Cr5NiMoV steel

X. J. Zhang<sup>1</sup>, M. V. Li<sup>2</sup>, K. Yang<sup>1</sup>, X. Y. Song<sup>1</sup>, L. Zhu<sup>1</sup>

(1. Tianjin Heavy Equipment Engineering Co., Ltd., China First Heavy Industries, Tianjin 300457, China;

2. Kunming University of Science and Technology School of Materials Science and Engineering)

272258170@163.com, limengnie@163.com

**Abstract:** Quantitative description of the isothermal diffusitive transformations is often made by the JMAK equation, and for the high alloy steel, the incubation time ( $t_s$ ) has to be considered, it was usually described as: The rule of additivity has been widely used to predict the phase transformation kinetics of steels during continuous cooling from JMAK isothermal data, but The JMAK equation can be applied with the additivity rule only if the rate of phase transformation ( $n$ ) depends only on the transformed volume fraction and the temperature. However, transformation rate is usually found very sensitive to the incubation time and the accuracy of the experiment, except for mechanisms of the phase transformation, the improper data treatment method can also lead to the variation. In this study, isothermal and continuous-cooling tests of 50Cr5NiMoV were conducted with the objectives of measuring the phase transformation kinetics of the austenite-pearlite and austenite-bainite reactions and validating the rule of additivity in 50Cr5NiMoV steel. The value of  $n$  were obtained from the experimental results, it was found that the value of  $n$  varies with the incubation time and the fitting methods. A new method to get a constant average transformation rate was developed, the method was used to get the JMAK parameters from the isothermal transformation experiments. The results showed that in the austenite-pearlite transformation, the  $n$  value can be set as a constant value 1, and the B value conformed a Gauss equation to temperature, while in the austenite-bainite transformation, the  $n$  value is 1.5, the B value are generally a Dosrep function of temperature. And then the overall isothermal austenite decomposition kinetics of the 50Cr5NiMoV roll steel with JMAK equation was made according to the isothermal dilation curves. The additivity rule was applied to predict austenite decomposition phase transformations in continuous cooling condition in this kind of steel, the accuracy of prediction was validated by the experimental continuous dilation curves. Furthermore, the coupled thermo-metallo model during the heat treatment process of the 50Cr5NiMoV back-up roll was made based on commercial ABAQUS software. The JMAK equation with additivity rule was applied in this model. In order to validate the model, the temperature history and microstructure distribution across the section of the back-up roll was measured experimentally. Temperature history were recorded by K-type thermocouples mounted on different locations of the back-up roll during the heat treatment process. The microstructure characteristics from surface to center along radial direction of the backup roll were carefully observed by optical microscopy (OM). Research findings showed that the predicted temperature agreed well with the experimentally measured temperature. The thermo-physical properties and thermal boundary conditions in the finite element model were valid. Predicted microstructure is in good agreement with the results of metallographic examination. The transformation kinetics and the material parameters were proved to be reasonable. It also indicated that the data treatment method and the phase transformation kinetics can be applied to predict solid phase transformation of high alloy steels.

**Keywords:** transformation kinetics, simulation, 50Cr5NiMoV, back-up roll

## **Three-dimensional numerical simulation of temperature field of Ni based cellular automaton modeling of nitriding process in pure iron**

Xiaohu Deng<sup>1</sup>, Dongying Ju<sup>2</sup>

(1. Tianjin University of Technology and Education; 2. Saitama Institute of Technology)

dengxh@tute.edu.cn

**Abstract:** A Cellular Automaton (CA) model has been developed to predict nitrogen concentration and microstructural evolutions in gas nitriding process of pure iron. The nitrogen diffusion was described by the Fick's Second Law and internal nitridation model, which can be solved using a central differential scheme. Moreover, a modified cellular automaton and Monte Carlo (MC) algorithm were employed to simulate the iron-nitrogen (Fe-N) phase transformation and grain growth. The diffusion model and phase transformation model are linked by the limiting nitrogen solubility and the effective diffusion coefficients. The phase fraction, grain morphology and orientation could be calculated by the model. In order to verify the model, gas nitriding process of pure iron was simulated under different nitriding process parameters. The simulated results agree well with available experimental ones and theoretical conclusions. Therefore, the comparison shows the reliability of the coupled model. It can be implemented to establish the processing-microstructure relation during the nitriding process.

**Keywords:** nitriding, cellular automaton, microstructural evolution, nitrogen diffusion, ironnitrogen phase

## **Design method fin-tube heat exchange based on numerical simulation**

Wenjing Yang, Yueming Xu, Peiwu Cong, Xinyu Zhou

(Beijing Research Institute of Mechanical & Electrical Technology)

wenjingyangbrimet@163.com

**Abstract:** Based on the basic principle and theory of heat transfer and fin-tube heat exchanger, design structure of fin-tube heat exchange to conform to the high pressure gas quenching process. Combined with numerical simulation and engineering experiment, heat exchange efficiency of the heat exchange under different initial conditions is simulated, according to the law of conservation of energy, the structure that satisfies the conditions and choose the most widely applicable structure. Measure temperature of delivery port, velocity of air intake and mass flow rate of water to get thermal power to compare with numerical simulation results, the result shows that: the experimental results coincide with numerical simulation, the structure can satisfy the high-pressure gas quenching process under various conditions, it is proved that the reliability of numerical simulation provides some technical support for the design of heat exchangers, which makes the design have some theoretical basis and provides new ideas for the optimization of other structures in the future.

**Keywords:** numerical simulation, law of conservation of energy, fin-tube heat exchanger, engineering experiment